DIRECT AMINO-TERMINATION OF NANODIAMONDS AND INVESTIGATION OF THEIR OPTICAL PROPERTIES UPON ANNEALING

Szabolcs CZENE[1,2], Olga KRAFCSIK[3,4], Nikoletta JEGENYES[2], Gábor BORTEL[2], Ádám GALI[2,3,5]

[1]Doctoral School on Materials Sciences and Technologies, Óbuda University, Bécsi út 96/b, H-1034 Budapest, Hungary, EU

[2]HUN-REN Wigner Research Centre for Physics, Institute for Solid State Physics and Optics, P.O. Box 49, H-1525 Budapest, Hungary, EU, czene.szabolcs@wigner.hun-ren.hu, gali.adam@wigner.hun-ren.hu

[3]Department of Atomic Physics, Institute of Physics, Budapest University of Technology and Economics, Műegyetem Rakpart 3, H-1111 Budapest, Hungary, EU

[4]HUN-REN Centre for Energy Research, Institute of Technical Physics and Materials Science, P.O. Box 49, H-1525, Budapest, Hungary, EU

[5]MTA-WFK Lendület "Momentum" Semiconductor Nanostructures Research Group, PO Box 49, H-1525, Budapest, Hungary, EU

https://doi.org/10.37904/nanocon.2025.5223

Abstract

Lattice defects in crystals serve as the base of quantum technologies. Among these, the nitrogen-vacancy (NV) center in diamond, particularly its negatively charged state (NV^-) has attracted considerable attention due to its stability at room temperature and potential application as a solid-state qubit. Nanodiamonds (NDs) are commonly synthesized by the high-pressure, high-temperature (HPHT) method. During post-synthesis cleaning, strong oxidizing acids (e.g., HNO_3, H_2SO_4, $HClO_4$) are employed, introducing various surface functional groups such as carboxyls. These surface groups can influence lattice defect sites and offer possibilities for further chemical modification. One such modification is Hofmann degradation, a well-known organic reaction that enables the direct formation of amino groups from carboxyl functionalities via decarboxylation. This process yields primary amine termination, which can facilitate the formation of C−N−C bonds, thereby favorably affecting NV^- center stabilization. Carboxyl- and amino-functionalized NDs were annealed at 600 °C, 750 °C, and 850 °C during 10 minutes. The NV^- fraction was measured using a Raman microscope. Significant temperature-dependent variations in this fraction ratio were observed. These differences are attributed to surface chemical transformations, as confirmed by infrared (IR) spectroscopy and X-ray photoelectron spectroscopy (XPS).

Keywords: Quantum technology, point defects, NV center, surface chemistry, spectroscopy

1. INTRODUCTION

The high-pressure high-temperature (HPHT) technique is a widely used method for producing NDs [1]. In this process, the diamond lattice forms from a carbon precursor under elevated pressure and temperature. Nitrogen is naturally present in the diamond lattice as an impurity and, in combination with a vacancy, forms NV center. The negatively charged (NV^-) and neutral (NV^0) states of this defect site are of particular interest. NV^- is especially significant for quantum informatics, as it serves as a stable quantum bit at room temperature [2]. To increase the concentration of NV centers, high-energy irradiation is used to create vacancies in the lattice, and ion implantation to increase the nitrogen content. Subsequent heating of the crystal enables vacancies to diffuse within the lattice and combine with nitrogen atoms to form NV centers [1]. The charge state of NV centers is influenced by several parameters e.g. by functional groups [3]. This surface effect is

limited to the centers located close to the surface [1]. Another commonly used technique is the detonation process. The detonation nanodiamonds (DNDs) are produced by detonation of N-containing compounds e.g. TNT. The DNDs contain higher concentration of sp^2 carbon due to the production and precursor material. Following the synthesis, NDs are purified and functionalized using strong acids such as $HClO_4$, $H2SO_4$, also HNO_3. In this oxidative environment, surface carbon atoms are oxidized, resulting oxygen-containing functional groups, carboxyl (-COOH), hydroxyl (-OH). These groups can be detected spectroscopically by IR and XPS [4]. The presence of these groups enables chemical modification of the surface and influences the NV^- fraction [3,5]. Amine termination has been achieved in various ways, including attachment of small molecules, plasma treatment [6,7]. The Hofmann degradation method is known in organic chemistry, and we previously applied it to silicon carbide nanoparticles to form NH_2 groups directly on the surface. This reference can be found among the citations of our previous publication at ref. 66 [8]. This reaction was also successfully utilized on NDs to investigate the effect of surface groups on the NV center [8]. The present study reports the results of the reactions induced by the heat treatment on directly amino-terminated NDs.

2. EXPERIMENTAL

Fluorescent ND samples (10, 30, 40, 50, 70, 90, and 140 nm FND/HPHT) and (30 nm DND) were purchased from Adámas Nanotechnologies. For the sample preparation, the as-received and previously reported amino-terminated samples [8] were placed in a hot furnace at 600, 750 and 850°C for 10 minutes in air. All analysis were performed on dry samples dried on Si substrate except at X-ray diffraction. The procedure to determine the NV^- fraction followed a previously published method [8]. Photoluminescence (PL) spectra were acquired using a Renishaw inVia Raman Microscope. The excitation wavelength for PL measurements was 532 nm, while Raman spectra were recorded using a 325 nm laser source. The IR spectra were measured by Bruker IFS66 spectrometer equipped with deuterated triglycine sulfate detectors. The X-ray Photoelectron Spectroscopy (XPS) measurements were carried out by an Escalab Xi^+ equipment (Thermo Fisher Scientific). A Microfocused monochromatic AlK_α x-ray gun was used, the radius of the analyzed area was 200 µm, while the base pressure of the analysis chamber was $3 \cdot 10^{-10}$ mbar. The X-ray diffraction (XRD) measurements were performed using a Huber G670 Guinier Imaging Plate Camera (Rimsting, Germany) with Cu Kα X-ray source (1.54 Å). The diffractograms were measured in the 10° to 100° 2θ range. The samples were placed in a glass capillary of 0.5 mm diameter and 0.01 mm wall thickness.

3. RESULTS AND DISCUSSIONS

It is hypothesized that annealing promotes further reactions of unreacted functional groups, such as formyl (−CHO), while the extended C−N−C bond and positive electron affinity reduce surface destabilization and significantly increase the NV^- fraction, which is important for quantum sensor applications [3,5]. Laura Dei Cas *et al.* demonstrated that significant graphitization does not occur during 10 minute period, even at elevated temperatures [9]. However, a temperature of 750°C is more than sufficient for phase transformation over a longer period, since it is above the reported 670°C threshold [10]. The NV^- fraction on the annealed samples is presented in **Table 1**.

Table 1 The NV^- fraction values in the case of as-received (COOH-terminated) and amino-terminated samples at different annealing temperatures. The applied laser power density was 2654 µW/cm^2.

	600°C		750°C		850°C	
size (nm)	COOH	NH_2	COOH	NH_2	COOH	NH_2
10	0.63(±0.10)	0.69(±0.07)	0.72(±0.12)	0.67(±0.15)	0.82(±0.04)	
30	0.68(±0.07)	0.81(±0.04)	0.76(±0.12)	0.85(±0.04)	0.71(±0.08)	0.73(±0.07)
40	0.60(±0.07)	0.67(±0.04)	0.77(±0.09)	0.77(±0.02)	0.73(±.09)	0.54(±0.06)

50	0.52(±0.04)	0.76(±0.09)	0.68(±0.12)	0.75(±0.07)	0.73(±0.09)	
70	0.58(±0.06)	0.80(±0.07)	0.60(±0.05)	0.65(±0.08)	0.60(±0.11)	0.65(±0.04)
90	0.60(±0.04)	0.77(±0.06)	0.74(±0.07)	0.57(±0.08)	0.74(±0.06)	0.66(±0.11)
140	0.59(±0.13)	0.84(±0.14)	0.74(±0.07)	0.73(±0.06)	0.69(±0.12)	0.71(±0.07)

The NH_2-terminated 30 nm, annealed NDs sample showed the highest NV^- fraction with small standard deviation at 750°C. To confirm reproducibility, we repeated the preparation and measurements from another batch of NDs. Since NV^- center quantity depends on laser power, we measured the 30 nm sample at multiple power levels and presented them in **Table 2** for two terminations. Similarly, to our previous publication [8], by increasing the laser power density, a degradation of the NV^- fraction is observed for the as-received NDs. However, a slight improvement is shown for the NH_2 compared to the COOH case, which can be attributed to converting the COOH into an amino group. Although the NH_2 group is attributed a negative electron affinity in the literature, it also has a stabilizing effect [5]. For NH_2 terminated NDs, changing the power keeps the NV^- constant within the standard deviation.

Table 2 The NV^- fractions at different laser power density and terminations measured on 30 nm NDs without annealing

laser power density (μW/cm²)	**177.7**	**320.6**	**1637.6**	**3135.9**
COOH terminated	0.63(±0.05)	0.63(±0.04)	0.61(±0.05)	0.58(±0.05)
NH_2 terminated	0.67(±0.03)	0.66(±0.04)	0.67(±0.04)	0.66(±0.04)

We reproduced the heat treatment with the new ND30 samples (**Table 3**). The value of NV^- fraction increased significantly in both cases as a result of the annealing, but more for the amino-terminated sample. The two surfaces show different trends. As laser power density increases a small improvement of the fraction can be measured with a much smaller standard deviation for the NH_2 sample, and the curve passes into saturation. At higher power, the measurements are limited by the sensitivity of the detector. In contrast, a stabilization is seen in the carboxyl-terminated sample from 1637 μW/cm² laser power density. The numerical data are given in **Table 2**.

Table 3 NV^- fraction in the case of 2 terminations after annealing measured at different laser power densities on 30 nm NDs

laser power density (μW/cm²)	**177.7**	**320.6**	**1637.6**	**3135.9**	**12682.9**
COOH annealed	0.71(±0.15)	0.75(±0.12)	0.78(±0.09)	0.78(±0.09)	0.77(±0.09)
NH_2 annealed	0.84(±0.03)	0.86(±0.03)	0.88(±0.03)	0.89(±0.03)	0.91(±0.03)

Surface groups, atoms influence the charge of defects. We first used IR spectroscopy to examine surface changes at 750°C, where the most favorable values were observed, and at 850°C, where a significant decrease in the negatively charged state occurred. The resulting spectra are presented in **Figure 1**.

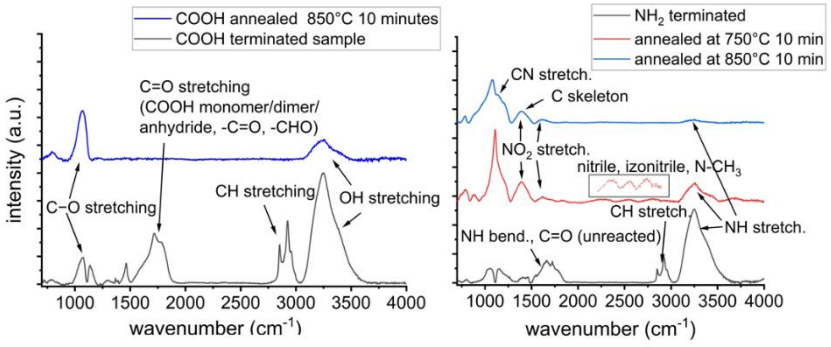

Figure 1 IR spectra of the COOH and NH_2 samples before and after annealing on 30 nm NDs

Since the NV^- values are quasi equal at high annealing temperatures for the COOH-terminated surface we present here the IR spectrum for 850 °C annealing. The annealing induced a common change in both terminated samples, the disappearance of CH bands. The absence of these bands contributes significantly to the increasing NV^-. The H-terminated surface markedly destabilizes the NV^- state in air through the band bending effect [5]. Another shared feature is the disappearance of carboxyl and carbonyl groups. These groups create acceptor states in the band gap, leading to quenching of the NV^- state.

The N-terminated surface proved more complex. On the one hand, residual COOH groups as well as formyl and keto groups may still be present. CH bands are apparently eliminated, though they may occur between 2700–2880 cm^{-1} due to Fermi resonance [4]. The resulting alkyl amines also have a stabilizing effect on the NV^- state. Upon heating in air, NH_2 groups are partially oxidized to NO_2 groups, as indicated by the relative decrease in the intensity of NH stretching and bending bands.

In the sharp region between 1000–1260 cm^{-1}, partially exposed Si and the corresponding Si–O bonds are observed in addition to several types of C–N stretching vibrations. NH_2 groups can form in situ from nitrile (C≡N) and isonitrile (N≡C). Isonitrile first converts to the more stable nitrile and can subsequently be reduced to amino groups at 750 °C [11]. At higher temperatures, NH stretching and deformation vibrations are markedly diminished. The broad band between 1270–880 cm^{-1} partially is attributed to Si−O, C−N and C−O bonds in different environments. The oxygen can form new C−O bonds, at both 750 and 850 °C, appearing at 1000–1200 cm^{-1} depending on the degree of order.

Since carbonyl groups are absent, the broad band between 3100–3470 cm^{-1} can be attributed to OH stretching vibrations. Our aim of achieving more favorable stabilization through the formation of C−N−C bonds was confirmed by IR analysis. To further corroborate these findings, we investigated the new bonding states by XPS. The C and N spectra are shown in **Figure 2**. Calibration was done to SiO_2, with positions fixed relative to each other within 1 eV, and the curves were fitted accordingly [12].

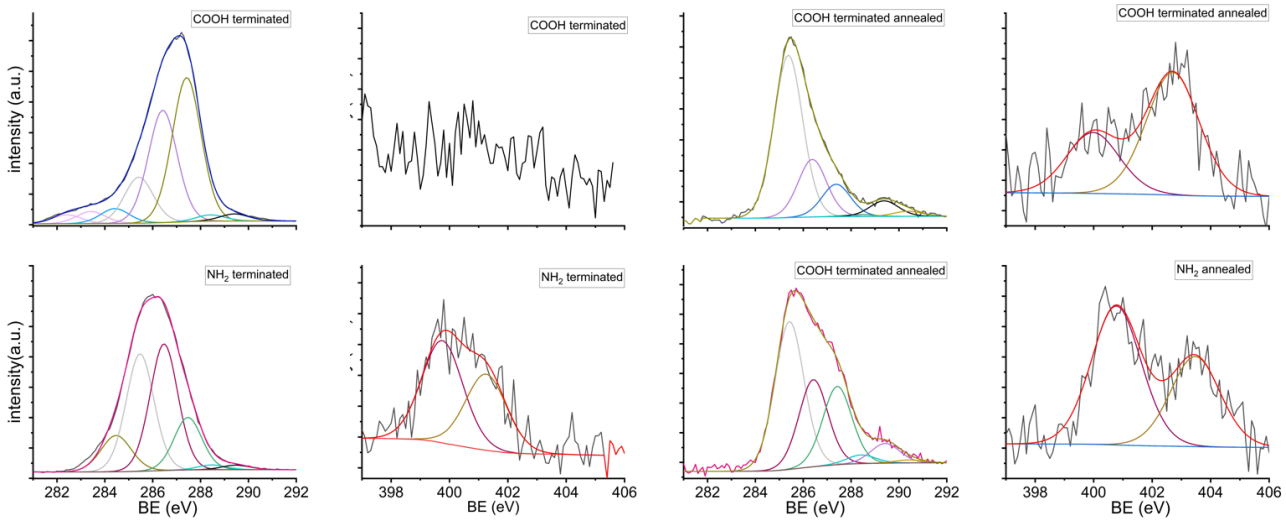

Figure 2 XPS spectra of the COOH and NH_2 samples before and after annealing on 30nm NDs

XPS spectra reveal another stabilizing effect: sp^2 carbon disappears after heating in both samples at 284.4 eV. Due to the higher conductivity of the sp^2/graphite layer, withdraws electrons from the NV^- state. In the amino-terminated sample, the main nitrogen-containing group is -NH_2, which is unstable and slowly oxidizes in air. The peak at 401.5 eV corresponds to the oxime (−NH−OH). After annealing the COOH-terminated sample, two nitrogen peaks appeared at similar positions as in the NH_2-terminated sample, but with different ratios. In the NH_2 sample, both species shifted to higher energies upon heating, indicating further oxidation while NH bonds remain. The peak at higher energy can be attributed to the appearance of NO_2 The

appearance of nitrogen after heating the COOH-terminated sample is notable. Although nitrogen is stable due to its triple bond, it can strongly adsorb and undergo charge transfer on surfaces with defects, vacancies, or dangling bonds, radicals [13]. This results in binding to the polar surface in a more oxidized state, which is partially reduced by hydrogen loss. Peaks below 284 eV are attributed to charging effects. To assess whether NH_2-termination offers protective effects against burning of the material, we prepared and annealed the DND30-NH_2. The COOH-terminated DND30 sample was centrifuged multiple times with pure water to remove all non-sedimented material. These samples have higher sp^2 carbon content than those prepared by the HPHT method. The NV center is not clearly detectable in the PL spectrum because its signal may overlap with the sp^2 C-related structures' emission. Notably, in the COOH-terminated DND sample, none of the 40 measured points showed NV center signals for annealed and not annealed cases. The PL signal of NV was observable for NH_2-terminated samples only after the annealing. The NV^- fraction value at 3135.9 μW/cm^2 is 0.71(±0.11) and at 12682.9 μW/cm^2 is 0.81(±0.03). **Figure 3** presents the PL spectra and Raman spectra of DND samples before and after heat treatment. The presence of the diamond peak and the reduction in graphite content were confirmed by the Raman spectra.

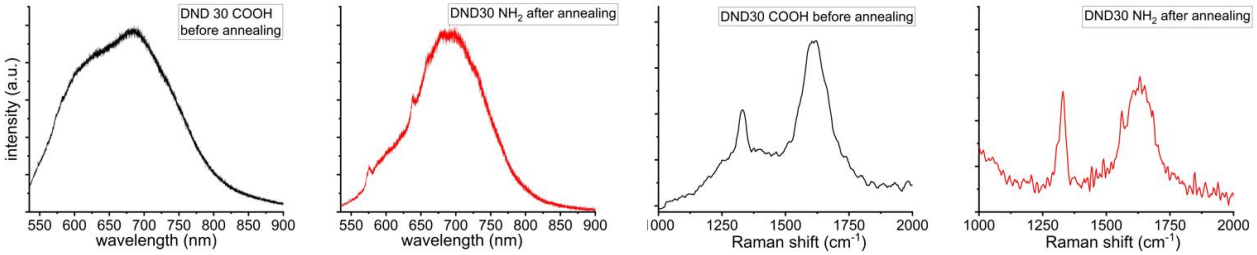

Figure 3 PL and Raman spectra of DND COOH and NH_2 before and after annealing

Graphite oxidizes much more readily than diamond, but at 750 °C even diamond is susceptible to oxidation. In this context, the NH_2 groups can exert a protective effect. As discussed above, C−N−C bonds are formed during the condensation reaction with adjacent carbonyl groups. The resulting secondary amines are more resistant to oxidation than surfaces terminated with oxygen-containing functional groups. This behavior is also reflected in the Raman spectra. After annealing the amino-terminated sample, the diamond peak at 1330 cm^{-1} and the graphite G band at 1630 cm^{-1} appear with nearly equal intensities, whereas in the COOH-terminated sample the G band is approximately 30% more intense.

The abundance of amino groups and the assumed protective effect depend on the reagent. Higher surface coverage and the corresponding enhanced protection were achieved starting from 5 mg DND30 and using 1 g NaOH and 1 ml Br_2 for the Hofmann degradation. We regained 0.5 mg from 3 mg annealed DND30-NH_2. In contrast, when DND30-COOH was annealed, the 96–97% of the material burned (35 mg → 1.2 mg). The residue was an orange, crystalline material, while the DND30-NH_2 annealed was slightly reddish. Energy-dispersive X-ray spectroscopy (EDX) revealed that the material was significantly enriched in Zr 0.16→13.06 atomic%, while the Zr content in the annealed DND30 NH_2 is 0.36%. X-ray diffraction (XRD) analysis identified the Zr source as ZrO_2, which is commonly used in grinding. Although diamond reflections are barely visible in the diffractogram, quantitative analysis of the crystalline phases by Rietveld analysis indicated 21% diamond (by weight). The amount of amorphous fraction was not quantified. The low visibility of diamond reflections in the diffraction pattern is due to the fact that the X-ray scattering intensity of elements scales with the square of the atomic number. Consequently, the scattering of heavier zirconium (Z = 40), will always dominate the diffraction pattern over the weaker diamond reflections (Z = 6).

CONCLUSION

The stabilization of the nitrogen-vacancy defect in the negative charge state upon illumination was achieved through annealing which is proven to be well pronounced compared to the previously demonstrated minor

degree of stabilization by other techniques. We found that the highest NV^- fraction can be obtained by annealing NH_2-terminated sample at 750°C. Spectroscopic analyses (IR and XPS) confirmed that stabilization arises from the formation of favorable C−N−C linkages, the removal of H termination, and a significant reduction in sp^2 carbon content. Experiments on detonation nanodiamond demonstrated that, during annealing, nitrogen has a protecting effect against burning of nanodiamonds. X-ray diffraction further revealed that a substantial portion of the crystalline phase consists of diamond, within which the NV^- state is present in appreciable proportions.

ACKNOWLEDGEMENTS

The work was supported by the Quantum Information National Laboratory sponsored by National Research, Development and Innovation Fund (NKFIH) Grant No. 2022-2.1.1-NL-2022-00004. The research reported in this paper and carried out at Wigner Research Centre for Physics is supported by the infrastructure of the Hungarian Academy of Sciences.

REFERENCES

[1] SCHIRHAGL, R.; CHANG, K.; LORETZ, M.; DEGEN, C. L. Nitrogen-Vacancy Centers in Diamond: Nanoscale Sensors for Physics and Biology. *Annual Review of Physical Chemistry.* 2014, vol. 65, pp. 83–105. Available from: https://doi.org/10.1146/annurev-physchem-040513-103659.

[2] WEBER, J. R.; KOEHL, W. F.; VARLEY, J. B.; JANOTTI, A.; BUCKLEY, B. B.; VAN DE WELLE, C. G.; Awschalom, D. D. Quantum Computing with Defects. *Proceedings of the National Academy of Sciences.* 2010, vol. 107, no. 19, pp. 8513–8518. Available from: https://doi.org/10.1073/pnas.1003052107.

[3] JANITZ, E.; HERB, K.; VÖLKER, L. A.; HUXTER, W. S.; DEGEN, C. L.; ABENDROTH, J. M. Diamond Surface Engineering for Molecular Sensing with Nitrogen—Vacancy Centers. *Journal of Materials Chemistry C* 2022, vol. 10, no. 37, pp. 13533–13569. Available from: https://doi.org/10.1039/D2TC01258H.

[4] COATES, J. Interpretation of Infrared Spectra, A Practical Approach. In: *Encyclopedia of Analytical Chemistry*. John Wiley & Sons, Ltd, 2006. Available from: https://doi.org/10.1002/9780470027318.a5606.

[5] KAWAI, S.; YAMANO, H.; SONODA, T.; KATO, K.; BUENDIA, J. J.; KAGEURA, T.; FUKUDA, R.; OKADA, T.; TANII, T.; HIGUCHI, T.; HARUYAMA, M.; YAMADA, K.; ONODA, S.; OHSIMA, T.; KADA, W.; HANAIZUMI, O.; STACEY, A.; TERAJI, T.; KONO, S.; ISOYA, J.; KAWARADA, H. Nitrogen-Terminated Diamond Surface for Nanoscale NMR by Shallow Nitrogen-Vacancy Centers. *Journal of Physical Chemistry. C* 2019, vol. 123, no. 6, pp. 3594–3604. Available from: https://doi.org/10.1021/acs.jpcc.8b11274.

[6] YU, Y.; YANG, X.; LIU, M.; NISHIKAWA, M.; TEI, T.; MIYAKO, E. Anticancer Drug Delivery to Cancer Cells Using Alkyl Amine-Functionalized Nanodiamond Supraparticles. *Nanoscale Advances.* 2019, vol. 1, no. 9, pp. 3406–3412. Available from: https://doi.org/10.1039/C9NA00453J.

[7] LAUBE, Ch.; RIYAD, Y. M.; LOTNIK, A.; LOHMANN, F. P.; KRANERT, C.; HERMANN, R.; KNOLLE, W.; OECKINGHAUS, Th.; REUTER, R.; DENISENKO, A.; KHANT, A.; ABEL, B. Defined Functionality and Increased Luminescence of Nanodiamonds for Sensing and Diagnostic Applications by Targeted High Temperature Reactions and Electron Beam Irradiation. *Materials Chemistry Frontiers.* 2017, vol. 1, no. 12, pp. 2527–2540. Available from: https://doi.org/10.1039/C7QM00241F.

[8] JEGENYES, N.; VERKHOVLYUK, V.; CZENE, S.; CSÁKI, A.; KRAFCSIK, O.; CZIGÁNY, Z.; BEKE, D.; GALI, A. Materials and Spin Characteristics of Amino-Terminated Nanodiamonds Embedded with Nitrogen-Vacancy Color Centers. *arXiv*. 17. 2. 2025. Available from: https://doi.org/10.48550/arXiv.2502.07706.

[9] DEI CAS, L.; ZELDIN, S.; NUNN, N.; TORELLI, M.; SHAMES, A. I.; ZAITSEV, A. M.; SHENDEROVA, O. From Fancy Blue to Red: Controlled Production of a Vibrant Color Spectrum of Fluorescent Diamond Particles. *Advanced Functional Materials.* 2019, vol. 29, no. 19, 1808362. Available from: https://doi.org/10.1002/adfm.201808362.

[10] XU, N. S.; CHEN, J.; DENG, S. Z. Effect of Heat Treatment on the Properties of Nano-Diamond under Oxygen and Argon Ambient. *Diamond and Related Materials.* 2002, vol. 11, no. 2, pp. 249–256. Available from: https://doi.org/10.1016/S0925-9635(01)00680-X.

[11] ASHEK-I-AHMED; et al. Facile Amine Termination of Nanodiamond Particles and Their Surface Reaction Dynamics. *ACS Omega.* 2019, vol. 4, no. 16, pp. 16715–16723. Available from: https://doi.org/10.1021/acsomega.9b00776.

[12] DUCROZET, F.; GIRARD, H. A.; LEROY, J.; LARQUER, E.; FLOREA, I.; BRUN, E.; SICARD-ROSELLI, C.; ARNAULT, J.-C. New Insights into the Reactivity of Detonation Nanodiamonds during the First Stages of Graphitization. *Nanomaterials.* 2021, vol. 11, no. 10, 2671. Available from: https://doi.org/10.3390/nano11102671.

[13] VALLEJO, E.; LÓPEZ-PÉREZ, P. A. Strong Chemical Adsorption of CO2 and N2 on a Five-Vacancy Graphene Surface. *Solid State Communications.* 2022, vol. 356, 114934. Available from: https://doi.org/10.1016/j.ssc.2022.114934.